Quantitative relationships between β-lactam molecular properties and β-lactam/AcrAB-TolC complex geometry as determinants of MDR efflux

Márcia Miguel Castro Ferreira and Rudolf Kiralj. *marcia@iqm.unicamp.br, rudolf@iqm.unicamp.br, http://lqta.iqm.unicamp.br*

Laboratório de Quimiometria Teórica e Aplicada (LQTA), Instituto de Química, Universidade Estadual de Campinas, Campinas SP, 13084-971, Brazil

THE OBJECTIVES OF THIS WORK

1) To predict the position and orientation of 16 β-lactam antibiotics in the central cavity of the multidrug efflux pump AcrB (a component of AcrAB-TolC membrane transporter) that exists in several Gram-negative bacteria → using only known molecular structures and calculated properties of drugs (β-lactams and four organic dyes: dequalinium, ethidium, ciprofloxacin, rhodamine 6G) and protein-drug (AcrB-organic dyes) complexes → no protein-drug complex geometry optimizations nor molecular dynamics simulations were performed;

2) To show that the β-lactams and the organic dyes, although structurally diverse, have properties in common that are responsible for their active efflux;

3) To use this similarity and the AcrB-organic dye complexes to predict AcrB-β-lactam geometry and to rationalize it → Quantitative Drug Structure – Complex Geometry Relationships + Exploratory Analysis.

THE AcrAB-TolC PUMP, ITS MULTIDRUG RESISTANCE (MDR) EFFLUX MECHANISM, AND ITS SUBSTRATES

1

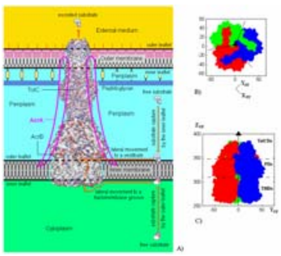

A): 3D & schematic representation of the AcrAB-TolC pump in *E. coli*. The two main drug efflux mechanisms start in the periplasm and cytoplasm. B), C): Blue, red and green AcrB protomers around the symmetry axis.

2

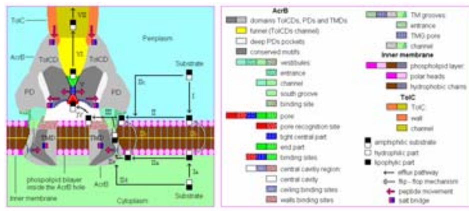

AcrB-mediated drug efflux from a Gram-negative cell in steps I - VII. Hydrophilic/lipophilic orientation of an amphiphilic drug is also visible. Conserved motifs, salt bridges and peptide movements are marked with special symbols. The efflux mechanism consists of a series of allosteric effects initiated by proton influx and contined by disruption of salt bridges and hydrogen bonds, changes in pump conformation, opening of efflux channels, drug binding in the central cavity and their extrusion through the pores and TolC.

3

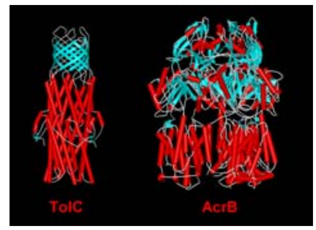

3D representation of the 3D structure of trimmers TolC (PDB: 1EK9, space group *R*3. V. Koronakis *et al.*, *Nature* 305, 2000, 914) and AcrB (PDB: 1IWG, space group *R*32. S. Murakami *et al.*, *Nature* 419, 2002, 587).

4

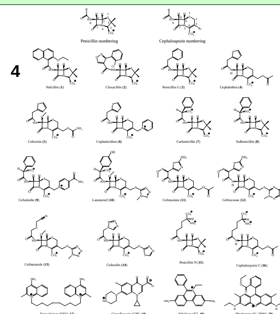

AcrAB-TolC substrates: β-lactam antibiotics (1-16) with atomic numbering, dequalinium (17), ciprofloxacin (18), ethidium (19) and rhodamine 6G (20).

RECEPTOR, SUBSTRATE AND RECEPTOR-SUBSTRATE COMPLEX FEATURES

5

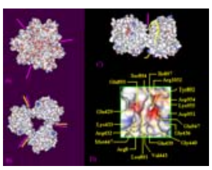

A) The pore domains (PDs) and (B) transmembrane domains (TMDs) viewed upwards and downwards the vestibules plane, respectively. C) The transmembrane groove (TMG) circular shape and position at the TMDs surface. The position of the vestibules (pink line) and of the TMGs (yellow circle). D) The TMG pore at its entrance, with essential residues.

6

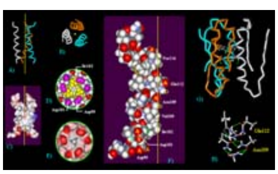

The pore channel viewed perpendicularly to (A) and along with (B) the symmetry axis. C) The pore channel interior excluding a helix. The pore recognition site by CPK (D) and electrostatic potential (E) model. F) A pore helix protomer by CPK model and with hydrogen bond (HB) donor (D's) and acceptor (A's) groups from residues (yellow) and the polypeptide chain (green). G) Three RND conserved motifs including the pore with HB residues that keep the pore to be tight. H) These residues with their HB network.

7

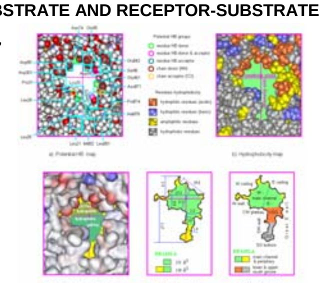

Vestibule and its 2D representation BRAMLA (BRAzil Map-Like Area). a) HB groups from residues and polypeptide chains. b) Hydrophobic character of the residues. c) The electrostatic potential map. d, e) BRAMLA area with its dimensions (d) and regions of its interior and exterior (e).

8

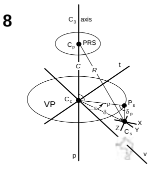

The AcrB-drug geometry parameters defined by the intersection of the vestibule axis (v) and protein symmetry axis (p). The distance and angle parameters are dependent variables that are quantitatively related to several steric and electronic molecular descriptors of drugs 1-20.

9

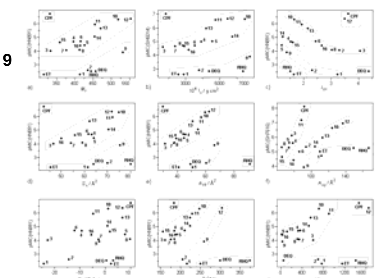

Representative efflux activity-drug molecular descriptor plots: a) pMIC(HN891) - M_r; b) pMIC(SH5014) - I_x; c) pMIC(HN891) - I_{yx}; d) pMIC(HN891) - S_x; e) pMIC(SH5014) - A_{yz}; f) pMIC(SH7616) - A_{xy}; g) pMIC(HN891) - D_y; h) pMIC(HN891) - α; i) pMIC(HN891) - |β_x|. See the table for definition of molecular descriptors calculated in this and previous work (M. M. C. Ferreira, R. Kiralj, *J. Chemometr.*, 18, 2004, 242-252).

PREDICTION OF β-LACTAM POSITION AND ORIENTATION IN THE CENTRAL CAVITY OF AcrB

10

List of molecular descriptors for drugs **1 - 20**

Symbol	Name and description	Nature[a]	Origin[b]	Ref.[c]
M_r	relative molecular mass	steric	compos	pw, tw
I_x	1st principal moment of inertia (around axis X)	steric	comput	pw, tw
I_y	2nd principal moment of inertia (around axis Y)	steric	comput	pw, tw
I_z	3rd principal moment of inertia (around axis Z)	steric	comput	pw, tw
I_{yx}	ratio between the principal moments I_y / I_x	steric	comput	tw
I_{zx}	ratio between the principal moments I_z / I_x	steric	comput	tw
I_{zy}	ratio between the principal moments I_z / I_y	steric	comput	tw
S_x	molecular area projected on the YZ plane (along X axis, in the CPK molecular model)	steric	molgrp	tw
$S_{\%}$	ratio between the area S_x and the area of the YZ face of the molecular box defined by the farthest CPK spheres (in the CPK molecular model), expressed as %	steric	molgrp	tw
α	molecular polarizability	electron	comput	pw, tw
|β|	absolute 2nd-order molecular polarizability β	electron	comput	pw, tw
|β_x|	absolute X component of β	electron	comput	pw, tw
γ	3rd-order molecular polarizability	electron	comput	pw, tw
D_x	X component of molecular dipole moment	electron	comput	pw, tw
D_y	Y component of molecular dipole moment	electron	comput	pw, tw
D_z	Z component of molecular dipole moment	electron	comput	pw, tw
n_x	surface molecular density projected on the YZ plane, defined as N / S_x, where N is the number of atoms	steric	molgrp	tw
Δ_1	the length of the molecular box along the axis X (in the CPK molecular model)	steric	molgrp	tw
Δ_{12}	the width(Y)/height(Z) ratio (of the YZ face of the molecular box (in the CPK molecular model)	steric	molgrp	tw
W_{Xm}	maximum of (X coordinate ± vdW radius)	steric	comput	tw
W_{YD}	difference between the maximum and mimimum of (Y coordinate ± vdW radius)	steric	comput	tw
W_{zy}	ratio between the W_{ZD} and W_{YD} differences	steric	comput	tw
A_{xy}	area of the XY face of the molecular box defined by the minimum and maximum atomic coordinates	steric	comput	tw
A_{yz}	area of the YZ face of the molecular box defined by the minimum and maximum atomic coordinates	steric	comput	tw
A_{xyz}	area of the molecular box defined by the minimum and maximum atomic coordinates	steric	comput	tw
Δ_{xy}	ratio between the X and Y edges of the molecular box defined by the minimum and maximum atomic coordinates	steric	comput	tw
Δ_{xz}	ratio between the X and Z edges of the molecular box defined by the minimum and maximum atomic	steric	comput	tw
Δ_{yz}	ratio between the Y and Z edges of the molecular box defined by the minimum and maximum atomic	steric	comput	tw

[a]Nature of molecular descriptors: steric or electron = electronic. [b]Origin or calculation method: compos = compositional, comput = computed and molgrp = molecular graphics descriptors. [c]Reference: tw - this work, pw - previous work.

11

Parameter	DEQ (17)	CPF (18)	ET (19)	RHQ (20)
C / Å	7.24	6.29	6.34	7.30
S_p / Å	2.64	7.20	8.28	15.02
δ / Å	8.20	14.94	9.72	17.29
ρ / Å	4.48	13.09	8.09	8.55
R / Å	10.85	18.80	15.48	23.91
A_{xv}	88.3°	73.0°	98.8°	87.2°
A_{yv}	70.3°	149.7°	73.1°	99.3°
A_{zv}	160.2°	65.7°	19.3°	9.8°
A_{xp}	151.0°	158.6°	82.5°	97.9°
A_{yp}	116.5°	110.8°	19.7°	168.2°
A_{zp}	100.9°	94.9°	71.5°	98.9°
ε	78.3°	4.0°	−11.4°	−1.4°
Π_{xp}	15.1°	77.4°	168.4°	171.7°
Π_{yp}	116.5°	111.0°	80.2°	82.8°
Π_{zp}	100.9°	155.2°	95.3°	85.9°
Π_{xyp}	100.9°	21.3°	96.1°	86.0°

UP: Experimental values of the dependent variables for the four drugs (DEQ, CPF, ET, RHQ).

RIGHT: Predicted values of the dependent variables for β-lactams 1-16.

12

Y	Regression equations[a]: $Y = a(\sigma_a) + b(\sigma_b)\,X_1 + c(\sigma_c)\,X_2$	R[b]	p[c]	Δ_{av}[d]	Predictions[e]: range	Predictions[e]: mean(sd)
C	$C = 5.84(30) + 0.000253(73)\,I_x$	0.926	0.074	0.15	6.2 - 7.1	6.5(3)
	$C = 5.47(40) + 0.00251(72)\,A_{xyz}$	0.927	0.073	0.15		
	$C = 4.79(36) + 0.0155(27)\,A_{xy}$	0.971	0.029	0.11		
S_p	$S_p = 24.20(216) - 5.48(72)\,\Delta_{xz}$	0.983	0.017	0.70	6.5 - 14.0	11.5(18)
	$S_p = 1.36(92) + 0.00517(58)\,\|\beta\|$	0.988	0.277	0.57		
	$S_p = 42.22(284) - 34.59(287)\,n_x$	0.993	0.007	0.49		
δ	$\delta = 26.04(697) - 4.90(231)\,\Delta_{xz}$	0.832	0.168	2.10	10.0 - 17.1	14.7(17)
	$\delta = 4.93(239) + 0.00511(151)\,\|\beta\|$	0.923	0.175	1.55		
	$\delta = 43.93(1184) - 32.76(1197)\,n_x$	0.888	0.112	1.76		
ρ[f]	$\rho = [\delta^2 - S_p^2]^{1/2}$	-	-	-	7.6 - 9.7	9.1(5)
R	$R = 33.09(533) - 5.45(177)\,\Delta_{xz}$	0.909	0.091	1.62	15.4 - 23.1	20.4(19)
	$R = 9.85(120) + 0.00553(76)\,\|\beta\|$	0.982	0.018	0.74		
	$R = 52.38(780) - 35.80(789)\,n_x$	0.955	0.045	1.05		
A_{xv}	$A_{xv} = 94.9(45) - 0.92(37)\,D_x$	0.871	0.129	4.2°	81° - 106°	94(7)°
A_{yv}	$A_{yv} = 81.3(60) + 1.7(3)\,D_y$	0.972	0.028	5.9°	60° - 120°	83(14)°
A_{zv}	$A_{zv} = 81.1(518) + 41.8(138)\,I_{zx}$	0.907	0.246	19.4°	29° - 69°	13(29)°
	$A_{zv} = 140.8(547) + 70.4(182)\,\Delta_{xz}$	0.939	0.124	19.2°		
A_{xp}	$A_{xp} = 434.7(825) - 235.3(619)\,I_{zy}$	0.937	0.063	10.3°	82° - 191°	151(31)°
A_{yp}	$A_{yp} = 415.5(129) - 212.2(866)\,\Delta_{12}$	0.866	0.134	20.7°	77° - 215°	146(36)°
	$A_{yp} = 310.2(1033) - 118.8(582)\,\Delta_{xz}$	0.822	0.178	24.2°		
	$A_{yp} = 185.5(1311) - 419.3(1878)\,W_{zy}$	0.845	0.293	21.1°		
A_{zp}	$A_{zp} = 189.6(483) - 73.9(362)\,I_{zy}$	0.822	0.178	5.6°	82° - 99°	92(5)°
	$A_{zp} = 107.6(135) - 0.000229(16)\,\gamma$	0.995	0.046	0.9°		
	$A_{zp} = 87.4(391) - 194.7(424)\,\log(W_{Xm})$	0.956	0.155	2.9°		
ε	$\varepsilon = -81.3(310) + 55.2(218)\,\Delta_{xy} + 13.5(33)\,(\Delta_{xy})^2$	0.998	0.239	1.5°	28° - 65°	1(24)°
	$\varepsilon = 69.4(80) - 98.2(109)\,W_{zy} + 199.0(69)\,(W_{zy})^2$	[illegible]	0.073	0.5°		
Π_{xp}	$\Pi_{xp} = 254.0(147) - 52.5(48)\,I_{yx}$	0.992	0.008	6.7°	44° - 162°	111(32)°
	$\Pi_{xp} = 294.4(270) - 49.8(72)\,I_x$	0.980	0.020	12.3°		
	$\Pi_{xp} = 737.3(511) - 10.1(8)\,S_x$	0.994	0.007	6.6°		
Π_{yp}	$\Pi_{yp} = 53.7(57) + 12.4(15)\,I_{zx}$	0.986	0.014	2.3°	77° - 116°	100(12)°
	$\Pi_{yp} = 253.9(373) - 117.8(280)\,I_{zy}$	0.948	0.052	4.3°		
Π_{zp}	$\Pi_{zp} = 415.7(1067) - 26.1(91)\,A_x - 0.180(165)\,(A_x)^2$	0.946	0.472	7.2°	74° - 182°	131(33)°
	$\Pi_{zp} = 416.3(1105) - 26.2(95)\,W_{YD} - 0.193(172)\,(W_{YD})^2$	0.942	0.463	7.4°		
Π_{xyp}	$\Pi_{xyp} = 93.4(15) + 1.8(1)\,D_x$	0.998	0.002	1.5°	54° - 115°	91(14)°

[a]Regression equations: Y – dependent variable (an AcrB–drug geometry parameter), a, b, c – regression coefficients, $\sigma_a, \sigma_b, \sigma_c$ – statistical errors of a, b, c, respectively, given in brackets for the last 1-3 digits of the regression coefficients, X_1 – molecular descriptor or its simple function (log term), X_2 – square term of molecular descriptor. X_1 and X_2 have units as in the previous table. [b]Correlation coefficient between experimental and calculated values of Y for 17-20. [c]Maximum Student test probability for the regression coefficients. [d]Average absolute deviation of calculated from experimental values of Y for 17-20. Units are Å or ° (degree) as in the previous table. [e]Predicted values of Y for 1-16, as obtained from particular regression equations and then averaged. The range and mean with standard deviation in brackets are given for these predictions. Units are Å or ° (degree) as in the previous table. [f]Expression based on geometrical relationships as defined in the corresponding figure.

13

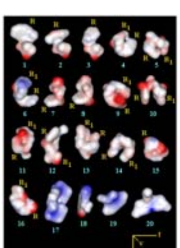

Most drugs expose positive, amphiphilic or hydrophobic heads (R, R_1) toward the predominantly negatively charged ceiling and pore.

14

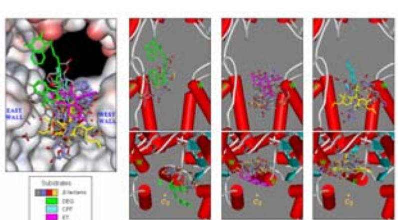

β-Lactams in predicted position/orientation in the central cavity, with experimental DEQ (green), CPF (light blue), ET (pink) and RHQ (yellow). Linear relationships between the dependent variables (protein-drug complex geometry parameters) and various electronic (dipole moment components, polarizabilities) and steric (principal moments of inertia and their ratios, molecular box size parameters) molecular descriptors of drugs 17-20 were established (see the tables). These relationships were then used to predict the orientational/positional parameters for the β-lactams. Three binding modes modes of the substrates in the central cavity were observed: predominantly E (east receptor wall) binding, W (west wall) biding, and bridging mode (two or more receptor sites are bound).

15

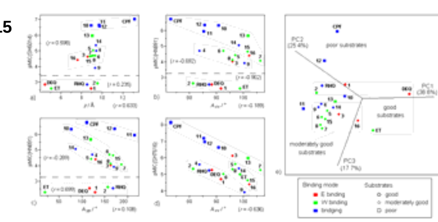

a)-d) Representative correlation plots between pMICs (efflux biological activities of AcrB in strains HN891 and SH5014 of *S. tiphymurium*) and AcrB-drug geometry parameters (calculated for 1-16, experimental for 17-20), with correlation coefficients for the complete data set and two subsets (separated by dashed midway line). e) 3D scores plot from PCA (Principal Component Analysis) for all dependent variables. The tendency of the sample clustering in terms of binding modes and activity classes may be observed by different coloring and legend.

16

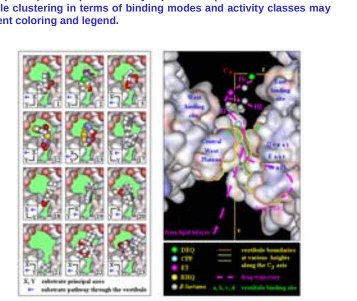

Left: Some drug molecules at the vestibule entrance, with deduced orientation of their XY axes, at qualitative level. Right: Probable drug efflux pathway portion. Experimental & predicted drug center of mass positions reveal four possible pathways: I - binding to the vestibule binding sites a-d; II - drug binding to the W binding site in the central hole; III - drug positioning in the middle of two or three binding sites; IV - binding to the E binding site. A drug molecule moves along these trajectories until reaching its best binding position.

ACKNOWLEDGEMENT: FAPESP